International Journal of Pure and Applied Physics.
ISSN 0973-1776 Volume 13, Number 1 (2017), pp. 101-107

http://www.ripublication.com

Study the Effect of Dopants on Structural and Electrical Properties of $BaTiO_3$ Perovskite Ceramics

Manoj Baloni

Department of Physics SGRR(PG) College Dehradun

Dehradun, Uttarakhand, India.

Abstract

Samples of $BaTi_{1-x}R_xO_3$ (where R= Mn; x =0, 0.2, 0.4, 0.6,0.8,) have been synthesized by solid-state reaction technique. No phase change in the crystal structure has been observed with Mn doping in barium titanate up to *x* = 0.8, however a decrease in crystallite size, lattice strain, *c*/*a* ratio and grain size has been found with Mn doping. The different results presented may be related to, and are explained by, the grain size and its distribution in the ceramic bulk. Mn doping in $BaTiO_3$ exhibit many interesting features, such as shift in transition temperature, increasing diffuse phase transition and decreasing dielectric constant. The evolution from a normal ferroelectric phase transition to a diffuse phase transition has been observed with increasing Mn concentrations. The dielectric study of samples poled in magnetic field suggests that T_c and maximum dielectric constant increase with increasing magnetic poling strength along with decreasing nature of diffusivity thus showing multiferroic nature.

INTRODUCTION

Multiferroics are known as materials exhibiting coupled electrical, magnetic, and structural order parameters, which can have simultaneously the ferroelectricity (with spontaneously ordered electric dipole moments), ferromagnetism (with

spontaneously ordered magnetic moments), and ferroelasticity (with spontaneously ordered strain arrangements). They are currently promising candidates applicable to electronic devices of high-speed nonvolatile memories, microelectro-mechanical systems, pyroelectric detectors, memory-cell capacitors, transducers, actuators, dielectric resonators, electromagnetic-interference filters, and so forth [1–12]. $BaTiO_3$ has a general ABO_3 type structure where A and B are cations of different sizes, with the 6 fold coordinate B cation in the middle, the 12 fold coordinate A cation in the corner and the anion, commonly oxygen, in the centre of the face. The packing of the ions can be thought of as the A and O ions together forming close-packed array. The phase of $BaTiO_3$ at room temperature is tetragonal and it transforms to cubic phase above 130ºC. It also exists in orthorhombic phase at 0ºC and in rhombohedral phase below -90ºC. Above 1460□C, $BaTiO_3$ exits in hexagonal phase . Although the primitive cube is the idealized structure, differences in radius between the A and B cations can alter the structure to a number of different so-called distortions, of which tilting is the most common one. With perovskite tilt the BO_6 octahedron twists along one or more axes to accommodate the difference. The ferroelectric properties of ABO_3 type perovskite ceramics (here barium titanate) can be efficiently controlled by doping with different doping elements.

Mn doped barium titanate materials in the bulk form are still explored over a wide range of compositions and controlled ion substitutions. Few reports are available on this issue where the micro-structural changes in Mn doped barium titanate[13], dielectric characteristics of Mn-ion doped $BaTiO_3$ nanoparticles[13] (Mn is doped at Ti-site), exaggerated grain growth in Mn doped $BaTiO_3$ (Mn concentration ~0.5 mol%) to study hexagonal phase in $BaTiO_3$ dielectric characteristics of BT co-doped[12] with Mn , electrical transport properties of Mn doped BT at high temperature[14], valence change and phase stability of Mn doped BT annealed in O_2 and H_2 are discussed[1]. In this paper, the synthesis, characterization and dielectric properties of Mn-doped BT have been studied and the effect of magnetic field on the dielectric properties of BNT has been analyzed.

SYNTHETIC PROCEDURE

$BaTi1–xR_XO3$ (where R= Mn; x =0, 0.2, 0.4, 0.6,0.8,0.10) were prepared by conventional method based on solid state reaction of mixed oxides, using required amount of analytical grade reagents $BaCO_3$, TiO_2, MnO as starting materials. The weighed individual reagents were homogeneously mixed in acetone media. The well-mixed powder was then calcined at 1200°C for 2 h, in alumina crucible. Calcined

powder was pressed into cylindrical pellets of 1-2 mm thick and 8 mm diameter at a pressure of ~31.2 × 10^6 Pa, using uniaxial hydraulic press. These pellets were then sintered at 1250°C for 5 h. Crystal structure and phase identification of the powder of sintered pellets was carried out by X-ray diffractometer (Brucker D8 Advance) using Cu-K_α radiation (λ = 1.5418 Å), the microstructure and the composition analysis were investigated using field emission scanning electron microscope (FE-SEM) with energy dispersion X-ray spectroscope attached (FEI, Quanta 200). The compositional analysis was carried out at different spots on the samples by applying accelerating potentials of 15 kV and 20 kV. Sintered pellets were polished and flat surface were coated with high purity silver paste and then dried at 120°C for 30 min, before taking electrical measurements. Dielectric measurements were conducted on an automated HIOKI 3532-50 Hi Tester, LCR meter. Dielectric permittivity were acquired in the frequency range 100 Hz - 1 MHz as a function of temperature (*T*) in a temperature range 35-200°C, where the sample undergoes the ferroelectric to paraelectric phase transition.

RESULTS AND DISCUSSION

X-ray diffraction (XRD) pattern of powder of all the sintered samples show that diffraction peaks occurred at slightly smaller angles when the specimens were doped with Mn ion and, although appreciable scatter existed in the *c*-axis values, the data did seem to indicate a lengthening of the *a*-axis and shortening of the *c*-axis to produce a more cubic structure with little change in cell volume. At first sight the XRD patterns of higher concentration of Mn^{+2} doped BT samples, could be thought that the patterns fit well with the peak position of Standard BT cube phase since splitting of cubic peak at 2θ=43.654 into tetragonal peaks (002) at 2θ = 44.853 and (200) at 2θ = 45.339 is not observed. However, from a more careful examination of the patterns, it is evidenced that the broadening of the peaks of a same diagram does not increase regularly with Bragg angle θ, i.e., does not obey to the Scherrer's equation[15]. This observation suggests that the lattices of the studied structures, initially cubic, have undergone a low tetragonal deformation. But the specimens do not show any phase involving the Mno compound up to x = 0.6 The linear particle size (L) and lattice strain (η) was calculated using following Scherrer's equation[15] and data is given in Table 1. $\beta_{1/2}\cos\theta = K\lambda/L+\eta\sin\theta$ where K = 0.89, $\beta_{1/2}$ is full width at half maxima. The lattice strain was calculated from slope of ν sinθ versus $\beta_{1/2}$ cos θ plot. From the data it is observed that Mn doping decreases the crystallite size, unit cell parameters and lattice stain in BT, which may be due to replacement of large ionic radii of Ba (r_6^{2+} = 1.35Å) ion by smaller ionic radii Mn (r_6^{2+} = 0.69Å) ion.

Table 1: Structural and dielectric properties of $Ba_{1-x}Mn_xTiO_3$

x	0	0.2	0.4	0.6
a (Å)	4.1120	4.1002	3.9960	3.9997
c (Å)	4.1130	4.1099	4.0120	4.0134
c/*a*	1.0024	1.0023	1.0040	1.0034
Crystallite size (nm)	33	32	30	29
Lattice strain	0.0173	0.0170	0.0102	0.0099
Grain size (μm)	3.2	2.8	1.05	0.99
γ	1.23	1.26	1.29	1.39
δ	30.10	36.25	40.79	46.10

The FE-SEM images of $Ba_{(1-x)}Mn_xTiO_3$ for x = 0, 0.2, 0.4, 0.6,0.8 respectively are shown in Fig. 1. From the SEM micrographs it is clear that grain distribution was uniform with least possibility of porosity throughout the sample's surface. Also the edges of the grains are not so sharp, which confirms the melting like nature of sample(Fig. 1 a-d), moreover this melting look was found to increase with Mn doping in BT. The average grain size was determined by classical linear interception method and the data is presented in Table 1. From the data it is found that grain size decrease with Mn doping..

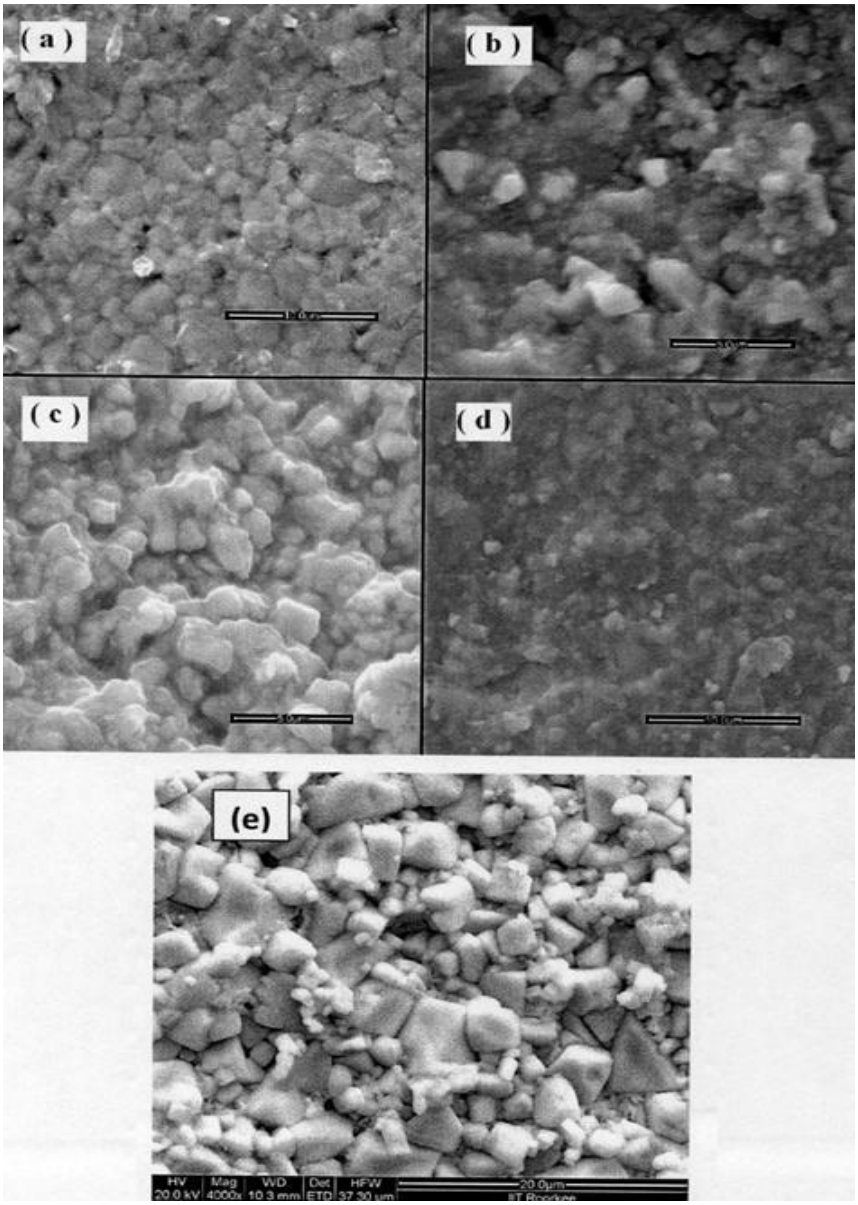

Fig. 1: FE-SEM images of $Ba_{1-x}Mn_xTiO_3$ (a) $x = 0.0$, (b) $x = 0.2$, (c) $x = 0.4$, (d) $x = 0.6$ and (e) $x = 0.8$

The variation of dielectric constant as a function of temperature for different Mn doped BT compositions at 1 kHz frequency show that the dielectric constant increases gradually with increasing temperature up to the transition temperature (T_c) and then it decreases. Here the region around dielectric peak is broadened which is one of the most important characteristics of disordered perovskite structure with diffuse phase

transition. This broadening is considered to be due to compositional fluctuations[8]. The position of transition temperature (T_c) found to shift towards lower temperature side with increase in the Mn concentration. It was also observed that dielectric peak maxima decreases with Mn doping, in general the *c*/*a* ratio indicates tetragonality distortion[16,17], i.e., higher the *c*/*a* ratio higher will be tetragonality distortion and hence high will be dielectric constant.

CONCLUSIONS

The system $Ba_{1-x}Mn_xTiO_3$ where x = 0, 0.2, 0.4, 0.6and ,0.8 was prepared by solid state reaction method. No phase change in the crystal structure was observed with Mn doping in BT, however a decrease in crystallite size, lattice strain, *c*/*a* ratio and grain size was found with Ni doping. All the different results presented may be related to, and are explained by, the grain size and its distribution in the ceramic bulk. Mn doping in $BaTiO_3$ exhibit many interesting features, such as shift in transition temperature, increasing diffuse phase transition and decreasing dielectric constant. The evolution from a normal ferroelectric phase transition to a diffuse phase transition was observed with increasing Mn concentrations. The dielectric study of samples poled in magnetic field suggests that T_c and maximum dielectric constant increase with increasing magnetic poling strength along with decreasing nature of diffusivity.

REFERENCES

[1] S. E. Park and T. R. Shrout, J. Appl. Phys. 82, 1804 (1997).

[2] M. Ozgul, E. Furman, S. Trolier-McKinstry, and C. A. Randall, J. Appl. Phys. 95,2631 (2004).

[3] V. Bornand, S. Trolier-McKinstry, K. Takemura, and C. A. Randall, J. Appl. Phys. 87,

[4] 3965 (2000).

[5] X. Qi, J. Zhou, B. Li, Y. Zhang, Z. Yue, Z. Gui, and L. Li, J. Am. Ceram. Soc. 87, 1848 (2004).

[6] W. M. Zhua, H. Y. Guoa, and Z. G. Ye, J. Mater. Res. 22, 2136 (2007).

[7] H. Zheng, J. Wang, S. E. Lofland, Z. Ma, L. Mohaddes-Ardabili, T. Zhao, L.

[8] Salamanca-Riba, S. R. Shinde, S. B. Ogale, F. Bai, D. Viehland, Y. Jia, D. G. Schlom, M. Wuttig, A. Roytburd, and R. Ramesh, Science 303, 661 (2004).

[9] H. A. Begum, H. Naganuma, M. Oogane, and Y. Ando, Materials 4, 1087 (2011).

[10] E. L. Colla, I. Stolichnov, P. E. Bradely, and N. Setter, Appl. Phys. Lett. 82, 1604 (2003).

[11] S. Valencia, A. Crassous, L. Bocher, V. Garcia, X. Moya, R. O. Cherifi, C. Deranlot, K.

[12] Bouzehouane, S. Fusil, A. Zobelli, A. Gloter, N. D. Mathur, A. Gaupp, R. Abrudan, F. Radu, A. Barthe´le´my, and M. Bibes, Nature Mater. 10, 753 (2011).

[13] J. Zhang, J. Zhai, and X. Yao, Scr. Mater. 61, 764 (2009).

[14] S. F. Wang, Y. C. Hsu, J. P. Chu, and C. H. Wu, Appl. Phys. Lett. 88, 042909 (2006).

[15] T. Chakraborty, S. Ray, and M. Itoh, Phys. Rev. B 83, 144407 (2011).

[16] Jana A & Kundu T K, *Mater Lett*, 61 (2007) 1544.

[17] Duverger E, Jannot B, Maglione M & Jannin M, *Solid State Ionics*, 73(1994) 139.

[18] Suryanarayana C & Grant Norton M, *X-Ray diffraction, a practical approach*, (Plenum Press New York and London), 1998.

[19] Yung P, Won Jae L & Kim Ho Gi, *J Phys Condens Matter*, 9 (1997) 9445.

[20] 17.Prasad K, Sati R, Choudhary S N, Choudhary R N P & Yadav K L, *J Mater Sci Lett*, 12 (1993) 561.